International Journal of Minerals, Metallurgy and Materials
Volume 27, Number 1, January 2020, Page 26
https://doi.org/10.1007/s12613-019-1858-x

Characteristics of the reduction behavior of zinc ferrite and ammonia leaching after roasting

Chao Wang, Yu-feng Guo, Shuai Wang, Feng Chen, Yu-jia Tan, Fu-qiang Zheng, and Ling-zhi Yang

School of Minerals Processing and Bioengineering, Central South University, Changsha 410083, China

(Received: 15 February 2019; revised: 27 May 2019; accepted: 3 June 2019)

Abstract: A novel method for recovering zinc from zinc ferrite by reduction roasting–ammonia leaching was studied in this paper. The reduction thermodynamic of zinc ferrite by CO was analyzed. The effects of roasting parameters on the phase transformation and conversion rate of zinc ferrite, and the leaching behavior of zinc from the reductive roasted samples by ammonia leaching, were experimentally investigated. The mineralogical phase compositions and chemical compositions of the samples were characterized by X-ray diffraction and chemical titration methods, respectively. The results showed that most of the zinc ferrite was transformed to zinc oxide and magnetite after weak reduction roasting. 86.43% of the zinc ferrite was transformed to zinc oxide under the optimum conditions: CO partial pressure of 25%, roasting temperature of 750°C, and roasting duration of 45 min. Finally, under the optimal leaching conditions, 78.12% of zinc was leached into the solution from the roasted zinc ferrite while all iron-bearing materials were kept in the leaching residue. The leaching conditions are listed as follows: leaching duration of 90 min, ammonia solution with 6 mol/L concentration, leaching temperature of 50°C, solid-to-liquid ratio of 40 g/L, and stirring speed of 200 r/min.

Keywords: zinc ferrite; reduction roasting; ammonia leaching; zinc extraction; zinc-bearing waste

1. Introduction

At present, there are almost 9 million tons of zinc-leaching residue annually produced around the world and about 0.8 million tons of zinc-containing electric arc furnace (EAF) dust annually produced in China. Zinc-leaching residue and zinc-containing EAF dust are the by-products of the zinc hydrometallurgical process and electric furnace steelmaking, respectively [1–2]. The produced and stacked zinc-leaching residue and EAF dust occupy large areas of land, cause serious environmental problems, and waste valuable zinc resources [3]. Thus, it is essential to recover zinc resources from EAF dust and zinc-leaching residue for the supply of zinc production and environmental protection.

Generally, zinc mainly exists in the form of zinc ferrite in zinc-leaching residue and zinc-containing EAF dust. Zinc ferrite ($ZnO{\cdot}Fe_2O_3$) is insoluble in mild acidic or alkaline conditions due to its stable crystalline structure. In addition, some research has indicated that zinc ferrite could be dissolved under pressurized and hot acid leaching conditions. However, a large number of iron oxides were also dissolved, which increased the complexity of subsequent iron precipitation processes and made the recovery of iron more difficult [4].

Several methods have been developed to treat zinc ferrite to solve this problem. One route is the conversion of insoluble zinc ferrite into soluble zinc-containing compounds after roasting with additives, so that zinc and iron could then be separated and recovered through the following methods: In general, the used additives included acid additives (sulfate), alkaline additives (calcium oxide), and neutral additives (halogenide) [5–7]. Zinc ferrite can be decomposed into zinc sulfate ($ZnSO_4$) and ferric sulfate ($Fe_2(SO_4)_3$) after sulfidation roasting; the decomposition products can then be selectively extracted by water [8–9]. Furthermore, during the calcified roasting process, zinc ferrite was converted into zinc oxide and calcium ferrite; the zinc could then be selectively leached by either ammonia or alkaline leaching [10–12]. Additionally, zinc ferrite was decomposed into zinc chloride and ferric oxide after halogenation roasting with ferric chloride

Corresponding authors: Yu-feng Guo E-mail: yfguo@csu.edu.cn; Feng Chen E-mail: csuchenf@csu.edu.cn

($FeCl_3$), so that zinc and iron could then be separated by water washing according to their differing solubilities [13]. However, a large amount of harmful gas was produced during the chloride roasting process, which limited its industrial application on a large scale.

As for the separation of zinc from the production after conversion, acid leaching, alkaline leaching, and ammonia leaching are considered as three conventional leaching methods. Although these three methods have different principles and reactions, the fundamental purpose is the transfer of zinc into the solution while iron and other substances remain as solid residue as much as possible. As mentioned above, acid leaching faces a high iron concentration in solvents. Havlik *et al*. [14] found that a low concentration of sulfuric acid could not only achieve the low amount of dissolved iron, but could also achieve a low zinc-leaching efficiency. Halli *et al*. [15] proposed recycling EAF dust with organic acid leaching after NaOH roasting. Under the optimized conditions, 100% of Zn vs. only 10% of Fe could be leached. Alkaline leaching has a better selective extraction than acid leaching. Chairaksa-Fujimoto *et al*. [12] leached zinc oxide from the CaO treated dust using NaOH solution and without any notable dissolution of iron and calcium. Ammonia leaching is widely used in hydrometallurgy of non-ferrous metal. Yang [16] prepared high-purity zinc from a secondary zinc resource in ammonia-ammonium aqueous solution, and found the solubility of zinc reached the top when $[NH_3]/[NH_4Cl]$ = 1. Wang *et al*. [17] found that the leaching process of zinc oxide ore by NH_3–NH_4Cl solution was controlled by diffusion of particle apertures, and the model of reactions conformed to the shrinking core model. Xia and Pickless [18] studied the behavior of decomposition of zinc ferrite in NaOH solution and found the dissolution reaction was as follows:

$$ZnFe_2O_4 + 2[OH^-] = ZnO_2^{2-} + Fe_2O_3 + H_2O \quad (1)$$

Zeydabadi *et al*. [19] introduced a way of extracting zinc from blast furnace flue dust following by sulfuric acid leaching, purification with ammonium jarosite, extraction, stripping, and electrodeposition. Turan *et al*. [20] introduced a multiple method to recycle zinc and lead from zinc plant residue by roasting with H_2SO_4, water leaching, and, finally, NaCl leaching. About 86% Zn and 89% Pb were recovered under optimal conditions.

In addition, a reduction roasting process was applied to decompose zinc ferrite. Zinc ferrite could be decomposed to ZnO and Fe_3O_4 after reduction roasting. The reduction roasting–sulfate leaching process for recovering zinc from zinc-containing leaching residue was reported by researchers [21–22]. However, the problem of dissolving zinc and iron simultaneously has not been solved due to the poor leaching selectivity of zinc sulfate solution. Moreover, the zinc and iron resources in the leaching residue could be separated and recovered by magnetic separation after reduction roasting [23–27]. Nonetheless, the separation of ZnO and Fe_3O_4 in the roasting products could not completely be achieved, which led to a low iron recovery rate. Therefore, the reduction roasting–ammonia leaching process proposed in this study is aimed at investigating the characteristics of the reduction behavior of zinc ferrite and ammonia leaching of the production after roasting.

2. Experimental

2.1. Materials

The key to recovering zinc from zinc-containing dust and zinc-leaching residue is to extract zinc from zinc ferrite. The extraction of zinc from real dust will be easy if the zinc extraction from zinc ferrite can be achieved. Zinc ferrite, an artificial ore produced by EAF steelmaking or zinc hydrometallurgy, does not exist in nature. Synthesis of zinc ferrite is carried out by roasting the compounds of zinc oxide and ferric oxide. The pure zinc ferrite used in this study was synthesized by the following steps: First, the analytical purity reagents ZnO and Fe_2O_3 powder were thoroughly mixed with 1:1 in a molar ratio in an agate mortar. Then, the mixture was placed into a corundum crucible and roasted in a muffle furnace at 1200°C for 4 h. The roasted mixture was leached by hydrochloric acid with a concentration of 1 mol/L for 1 h at room temperature to remove the unreacted oxides. The leaching residue was roasted in the muffle furnace at 1200°C for 1 h. Finally, the second roasted product (<75 μm) was dried at 105°C for subsequent analysis and experiments. The X-ray powder diffraction patterns of synthetized zinc ferrite powder are shown in Fig. 1. It can be seen that the main phase of synthetized zinc ferrite was $ZnFe_2O_4$, and no impurity phase could be observed. The main peaks of the synthetic zinc ferrite in Fig.1 had the same 2θ scales as the zinc ferrite in EAF dust and zinc-leaching residue [21,28]. The total zinc and total iron of this synthetized zinc ferrite were 26.94wt% and 46.61wt%, respectively, which was close to the corresponding theoretical values of zinc ferrite, 27.12wt% and 46.33wt%. This signified that the synthetized zinc ferrite had enough purity for the following investigation.

2.2. Reduction roasting

Fig. 2 illustrates the schematic diagram of the shaft fur-

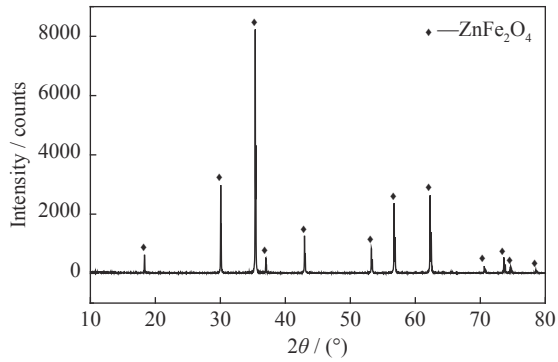

Fig. 1. XRD patterns of synthetized zinc ferrite.

nace with silicon carbide heating elements and an automated temperature control system. The synthetic zinc ferrite powder (2.5 g) was mixed with a small amount of water and pressed to form cylindrical pellets (ϕ10 mm × 10 mm). Ten dried pellets were placed into the quartz tube, and the furnace was heated to the designated temperature. After flushing with high-purity N_2 gas (>99.999%) for 20 min, the quartz tube was lowered into the shaft furnace and kept in the hot zone of the furnace. The N_2 gas was then replaced by the mixed gas of CO (>99.99%) and CO_2 (>99.99%) to conduct the reduction of zinc ferrite. After the required roasting duration was achieved, the gas was changed to N_2 gas until the roasted zinc ferrite cooled to room temperature. The flow rate of gas was kept at 8 L/min. At last, the roasted pellets were removed from the quartz tube for analysis and subsequent ammonia leaching experiments.

In addition, the aim of the reduction roasting was to decompose and transform the insoluble zinc ferrite to soluble

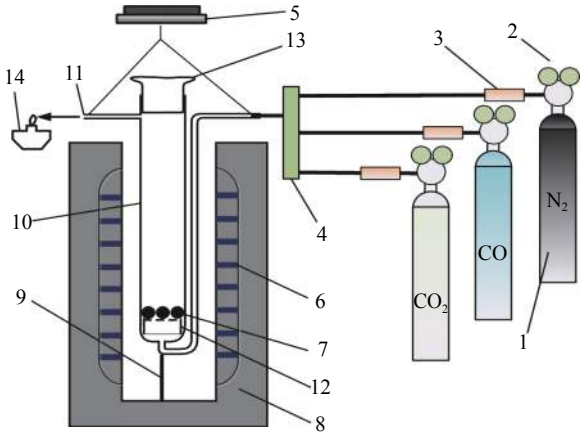

Fig. 2. Schematic diagram of the shaft furnace for reduction experiments. 1—Gas cylinder; 2—Pressure reducing valve; 3—Gas flowmeter; 4—Mixer; 5—Elevator; 6—Heating elements; 7—Sample; 8—Shaft furnace; 9—Thermocouple; 10—Quartz tube; 11—Gas outlet; 12—Perforated screen plate; 13—Ground quartz cover; 14—Alcohol burner.

ZnO and Fe_3O_4 so that the zinc and iron could be selectively leached and separated by subsequent ammonia leaching. Theoretically, it can be inferred that the more zinc ferrite transforms to zinc oxide during the reduction roasting, the more zinc and iron can be recovered by later ammonia leaching. Therefore, the results of reduction roasting were evaluated by the following indices:

The conversion ratio of zinc oxide (ω) could be obtained as in Eq. (2).

$$\omega = \frac{\gamma_1(\mathrm{Zn})}{\gamma_2(\mathrm{Zn})} \times 100\% \tag{2}$$

where $\gamma_1(\mathrm{Zn})$ is the mass percentage of zinc in the form of zinc oxide in the reduced sample, wt%; $\gamma_2(\mathrm{Zn})$ is the percentage of total zinc in the sample, wt%.

The percentage of ferrous content in total iron content (η) could be obtained as in Eq. (3).

$$\eta = \frac{\gamma(\mathrm{Fe}^{2+})}{\gamma(\mathrm{TFe})} \times 100\% \tag{3}$$

where $\gamma(Fe^{2+})$ is the percentage of ferrous in the reduced sample, wt%; γ(TFe) is the percentage of total iron in the sample, wt%.

2.3. Ammonia leaching

The ammonia leaching experiments of the reduction-roasted samples were carried out, and the schematic diagram of the apparatus is illustrated in Fig. 3. During the leaching process, the reduced roasted powder (≤75 μm) was dried at 110°C for 3 h. The leaching experiments were carried out in a 250 mL beaker in a water bath at constant temperature. 100 mL leaching solution was prepared in the 250 mL beaker sealed with plastic film according to the preset total

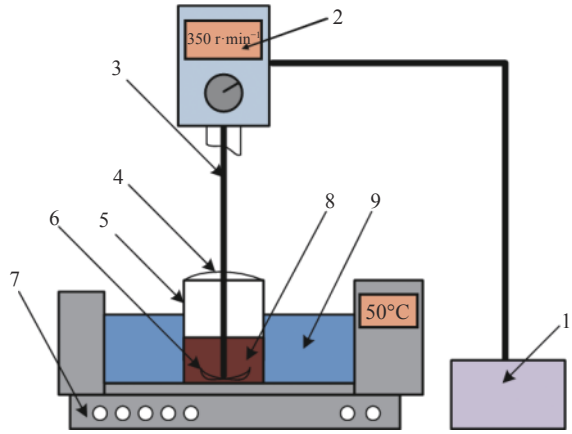

Fig. 3. Schematic diagram of the leaching experiment equipment. 1—Frequency converter stirrer bracket; 2—Agitator; 3—Stainless steel impeller; 4—Plastic film; 5—Beaker; 6—Stirring blades; 7—Constant temperature water bath; 8—Sample and ammonia mixture; 9—Constant temperature flume.

ammonia concentration and the ratio of ammonia and ammonium. Then, a certain amount of reduced roasted powder was placed into the beaker. The agitator started stirring when the required experimental temperature of the water bath was reached. After the required leaching duration ended, the leachate was separated from the residue by vacuum filtration and analyzed.

The leaching ratio of zinc (R), which is the maximal theoretical value of zinc-leaching rate by ammonia leaching, is calculated as in Eq. (4):

$$R = \left(\frac{C \times V}{G \times W}\right) \times 100\% \quad (4)$$

where C is the concentration of zinc in the filtrate, g/L; V is the volume of filtrate, L; G is total mass of the sample, g; W is the zinc content of the sample.

2.4. Characterization techniques

Potassium dichromate titration for total Fe, and ferrous and EDTA titration for Zn were performed for the chemical analysis of reduction products and leaching residue according to the Chinese standard GB/T 6730.65–2009, GB/T 8151.1–2012, and GB/T 6730.8–2016.

The mineral phase compositions of the samples were determined by XRD (Japan, TTR-III, D8 Advance) with a graphite monochromator and Cu-Kα radiation in the range of 20–80° at a scanning rate of 10°/min. The content of zinc in the leachate was determined by inductively coupled plasma mass spectrometry (ICP-MS) (Thermo Fisher Scientific, ICAP7400 Radial). In addition, the content of zinc oxide in the roasted products was analyzed by leaching with 5vol% acetic acid at 100°C for 1 h to extract zinc oxide, which could be determined by ICP-MS method subsequently [29].

3. Thermodynamic analysis

For this step, the reduction thermodynamic of zinc ferrite during the reduction roasting process was calculated using FactSage 7.0. The temperature range for the thermodynamic calculations was from 500 to 1100°C. The results are listed in Table 1.

Eq. (5) in Table 1 shows that zinc ferrite ($ZnFe_2O_4$) is easily reduced to ZnO and Fe_3O_4. Moreover, it can be seen that the formed Fe_3O_4 and ZnO can be reduced to FeO, Fe, and Zn under a strong reduction atmosphere and high temperature. Therefore, in order to clear the effects of reductive atmosphere and temperature on the reduction thermodynamic, the equilibrium phase compositions of the zinc–iron–oxygen system were calculated at different temperatures and different reductive atmospheres according to the equations listed in Table 1.

Table 1. $\Delta G^{\ominus}$–T **calculations of relevant reactions**

Equation No.	Chemical reaction	$\Delta G^{\ominus}$ / (KJ·mol^{-1})	T / K ($\Delta G^{\ominus} = 0$)
(5)	$3ZnFe_2O_4 + CO = 3ZnO + 2Fe_3O_4 + CO_2$	$\Delta G^{\ominus} = 10.658 - 0.0556T$	191.7
(6)	$Fe_3O_4 + CO = 3FeO + CO_2$	$\Delta G^{\ominus} = 11.426 - 0.0215T$	531.4
(7)	$FeO + CO = Fe + CO_2$	$\Delta G^{\ominus} = -12.454 + 0.0225T$	553.5
(8)	$Fe_3O_4 + 4CO = 3Fe + 4CO_2$	$\Delta G^{\ominus} = -25.937 + 0.046T$	563.8
(9)	$ZnO + CO = Zn + CO_2$ (500°C < T < 900°C)	$\Delta G^{\ominus} = 67.455 - 0.0208T$	—
(10)	$ZnO + CO = Zn + CO_2$ (900°C < T < 1100°C)	$\Delta G^{\ominus} = 155.17 - 0.1175T$	1320.6

Note: $\Delta G^{\ominus}$ is the Gibbs free energy, T is the temperature.

The equilibrium phase compositions of the zinc–iron–oxygen system at different partial pressures of CO (P_{CO}/P_{CO+CO_2}) and temperatures are shown in Fig. 4. There are five phase areas in Fig. 4, including $ZnFe_2O_4$(s), Fe_3O_4(s) + ZnO(s), FeO(s) + ZnO(s), Fe(s) + ZnO(s), and Fe(s) + Zn(g). To achieve successful separation in the subsequent ammonia leaching process, the target area of reduction roasting of zinc ferrite should be Fe_3O_4(s) + ZnO(s), as marked in Fig. 4. As the temperature increased, the upper limit of CO partial pressure of the shadow area in Fig. 4 showed a gentle decrease. Thus, the higher roasting temperature required a lower CO partial pressure and had a better kinetic condition. According to the reduction production (Fe_3O_4(s) + ZnO(s)) and kin-

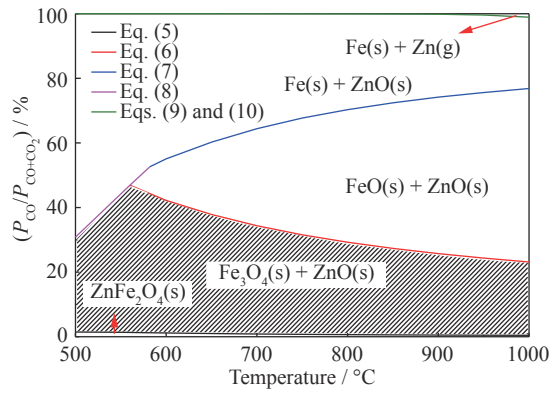

Fig. 4. Equilibrium phase compositions for reduction of zinc ferrite.

etics, the roasting temperature and partial pressure of CO were performed at the range of 600 to 900°C and 5% to 30% respectively during reduction roasting experiments in this study.

4. Results and discussion

4.1. Reduction roasting of zinc ferrite

4.1.1. Mineralogical variation after the reduction roasting

According to the above thermodynamic analysis, the decomposition of zinc ferrite during the reduction roasting process can be controlled to form ZnO and Fe_3O_4 by adjusting the temperature and partial pressure of CO. The XRD results of reduced samples under various roasting temperatures, partial pressures of CO, and roasting durations are shown in Fig. 5.

The effects of roasting temperature were studied at a fixed CO partial pressure of 25% and roasting duration of 60 min. Fig. 5(a) shows that the characteristic peaks of zinc oxide (ZnO) were observed when the roasting temperature reached 600°C, and its intensity presented a rising tendency with increasing roasting temperature. Furthermore, the peak position of zinc ferrite ($ZnFe_2O_4$) moved to magnetite (Fe_3O_4) [30]. The results were consistent with the previous report [31]. As the roasting temperature reached 800°C, FeO was detected in the samples. However, FeO very easily reacted with ZnO to form a new kind of spinel phase ($Fe_{0.85-x}Zn_xO$) at 900°C, which was hard to dissolve in acid and alkaline [32]. Thus, in order to avoid the formation of $Fe_{0.85-x}Zn_xO$, we found that the reduction roasting temperature should be kept below 800°C.

Figs. 5(b) and 5(c) show the effects of the partial pressure of CO and roasting duration on the phase compositions of reduced samples, respectively. Similarly, when the reduction potential becomes stronger, the decomposed product compositions of the zinc ferrite obeyed the following route: $ZnFe_2O_4 \rightarrow ZnO + Fe_3O_4 \rightarrow ZnO + FeO/Fe_{0.85-x}Zn_xO$.

The effect of the partial pressure of CO was investigated at a fixed temperature of 750°C and duration of 60 min. Fig. 5(b) shows that the FeO formed when P_{CO}/P_{CO+CO_2} reached 30%. The effect of roasting duration was investigated at a fixed temperature of 750°C and CO partial pressure of 25% and the results were showed in Fig. 5(c). Fig. 5(c) shows that ferrous oxide and a new spinel phase appeared when the roasting duration was up to 120 min.

These results were consistent with the thermodynamic analysis and indicated that selective reduction of zinc ferrite could be achieved by controlling reduction conditions: roasting temperature, P_{CO}/P_{CO+CO_2}, and roasting duration.

4.1.2. Effect of reduction roasting on the behavior of iron

According to Eq. (5) in Table 1, the theoretical percentage of Fe^{2+} in the total iron was 33.3wt% when the zinc ferrite ($ZnFe_2O_4$) completely decomposed to ZnO and Fe_3O_4. The percentage of Fe^{2+} in the total iron of the samples was chosen as an index to evaluate the results of reduction roasting. The target iron phase in the selective reduction production could be estimated by the percentage of Fe^{2+} in Total Fe. The value of η in magnetite was 33.3wt%; therefore, it could be regarded as an over reduction if the value of η were over 33.3wt%. Otherwise, it could be regarded as an insufficient reduction.

As shown in Fig. 6(a), the value of η increased with increasing roasting temperature under different reduced atmospheres and a constant roasting duration of 60 min. This could be explained as the increase in roasting temperature accelerating the reduction of zinc ferrite [33]. Fig. 6(b) shows the effect of roasting duration on the value of η at 750°C in 25% CO partial pressure. The values of η increased dramatically from 3.89wt% to 27.71wt% as the roasting duration increased from 0 to 30 min. Also, the value of η is 32.62wt%, which was the closest point to 33.3% when the roasting duration reached 75 min, meant that most of the $ZnFe_2O_4$ decomposed to ZnO and Fe_3O_4.

Furthermore, the values of η which were closest to 33.3wt% in different reduction roasting conditions are listed in Table 2. It should be noted that when CO partial pressure was < 15%, the value of η could not reach 33.3wt%, even though the roasting temperature was up to 900°C.

4.1.3. Effect of reduction roasting on the behavior of zinc

The aim of reduction roasting of zinc ferrite in this study was to decompose zinc ferrite to zinc oxide and magnetite. Therefore, the conversion rate of zinc is an important index to evaluate the result of reduction roasting. The effects of roasting temperature, roasting duration, and partial pressure of CO on the conversion rate of zinc ferrite after reduction roasting are shown in Fig.7.

Fig. 7(a) shows that most of the curves had an increasing trend with increasing roasting temperature when the temperature was below 750°C. The conversion ratios of zinc decreased with a further increase in roasting temperature from 750 to 900°C except for the curve of 5% CO partial pressure. It is well accepted that increasing roasting temperature and partial pressure of CO can promote reduction reactions. According to Eq. (5), the reduction of zinc ferrite resulted in the increase in conversion ratio of zinc. However, the FeO would form under strong reduction conditions so as to decrease the conversion ratio of zinc at higher temperatures and higher partial pressure of CO. Combining the XRD patterns in

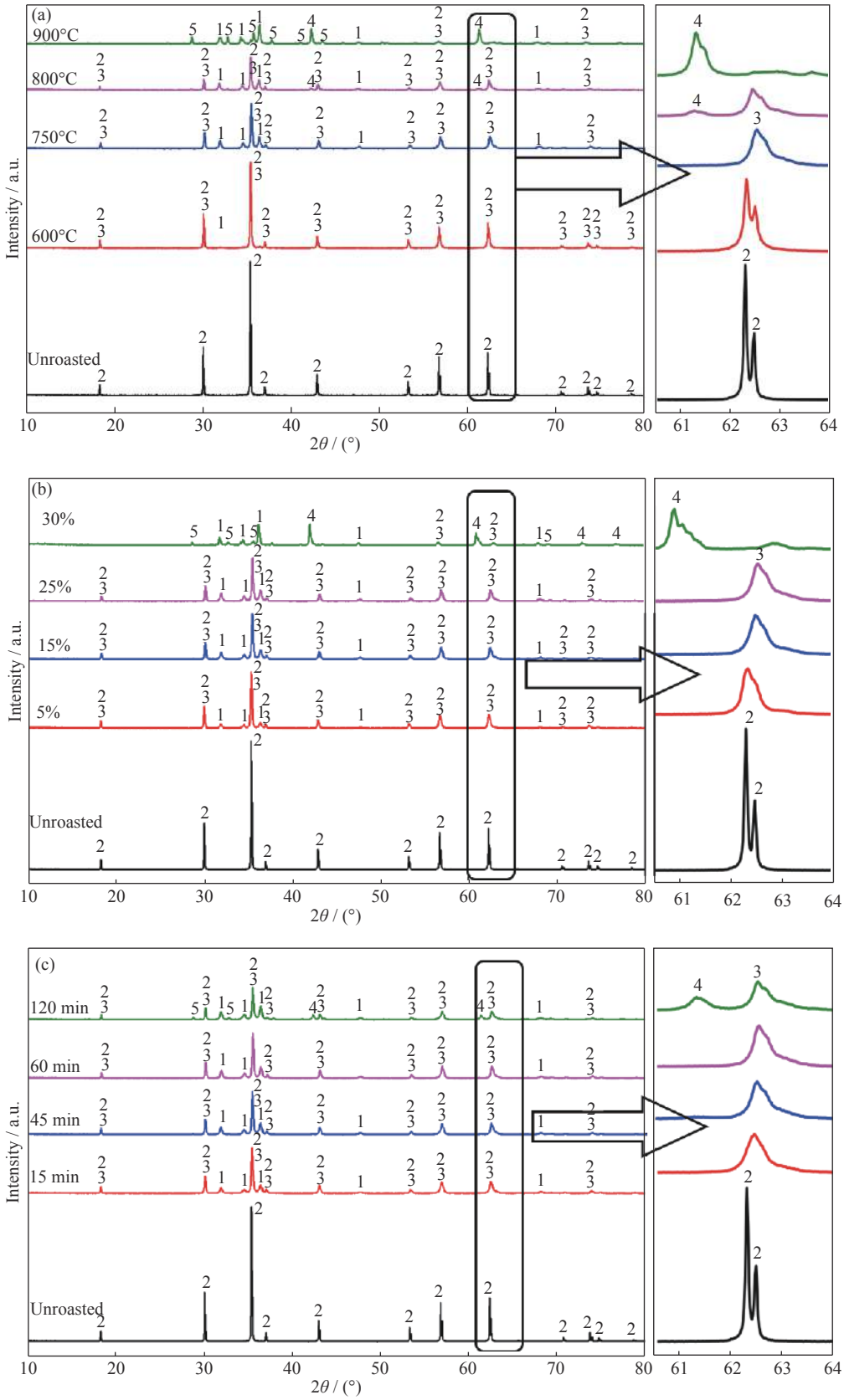

Fig. 5. XRD patterns of reduction roasting samples at different roasting temperatures (a), CO partial pressures (b), and roasting durations (c). 1—ZnO; 2—$ZnFe_2O_4$; 3—Fe_3O_4; 4—FeO; 5—$Fe_{0.85-x}Zn_xO$.

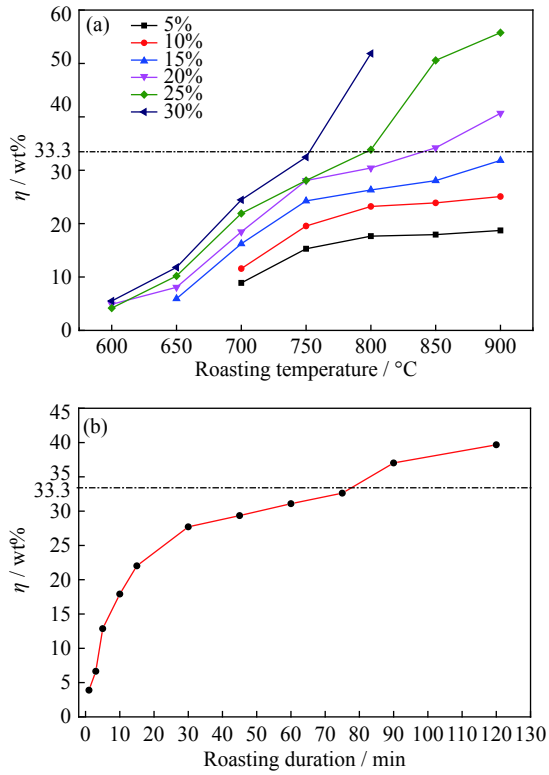

Fig. 6. Effect of roasting conditions on the percentage of ferrous content in total iron content (η): (a) temperature and CO partial pressure (roasting duration = 60 min); (b) duration (temperature = 750°C, CO partial pressure = 25%).

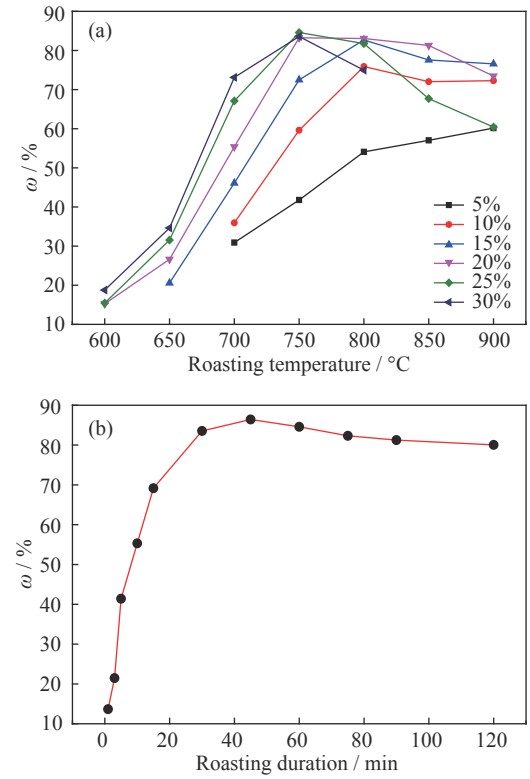

Fig. 7. Effect of roasting conditions on the conversion rate of zinc ferrite: (a) temperature (roasting duration = 60 min); (b) duration (temperature = 750°C, CO partial pressure = 25%).

Table 2. Values of η closest to 33.3% under different reduction roasting conditions

Reduction duration / min	Reduction temperature / °C	CO partial pressure / %	η / wt%
60	900	15	31.84
60	850	20	34.20
60	800	25	33.83
60	750	30	32.45
75	750	25	32.62

Fig. 5, the formed FeO from over reduction of Fe_3O_4 could react with ZnO to generate a kind of solid solution with sparing solubility in the leaching solution and led to a lower zinc conversion ratio [27].

The effect of roasting duration on the zinc conversion ratio was studied under conditions of 750°C with 25% CO partial pressure, as shown in Fig. 7(b). The conversion ratio of zinc increased rapidly with increasing roasting duration and reached 86.43% at 45 min. However, there was a slow decreasing trend in the conversion ratio of zinc ferrite with a roasting duration > 45 min. It could be explained by the generation of solid zinc solution ($Fe_{0.85-x}Zn_xO$) under the longer roasting duration.

In summary, the optimum reduction roasting parameters should be a roasting temperature of 750°C, CO partial pressure of 25%, and a roasting duration of 45 min. The maximum conversion ratio of zinc ferrite could reach 86.43% under optimal conditions.

4.2. Ammonia leaching of reduction-roasted product

4.2.1. Effect of leaching condition

Ammonia leaching is widely used in zinc extraction. Some researchers [16] have found that the NH_3–NH_4Cl ammonia system has an excellent ability to dissolve zinc oxide from zinc ores as $[NH_3]/[NH_4Cl] = 1$. In this step, the NH_3–NH_4Cl solution was applied to selectively dissolve zinc in the solution and to leave the iron in the residue. Therefore, the successful separation of zinc and iron in the reduced products could be achieved. The roasted zinc ferrite sample was prepared under a roasting temperature of 750°C for 45 min with a CO partial pressure of 25%. The effects of total ammonia concentration, leaching time, leaching temperature, solid-to-liquid ratio (S/L), and stirring speed on the zinc-leaching rate are shown in Fig. 8.

As shown in Fig. 8(a), the zinc-leaching rate had a sharp increase from 27.43% to 71.53% with increasing total ammonia concentration from 3 to 6 mol/L under the following leaching conditions: a 40 g/L of solid-to-liquid ratio, 60 min of leaching time, a 25°C of leaching temperature, and a

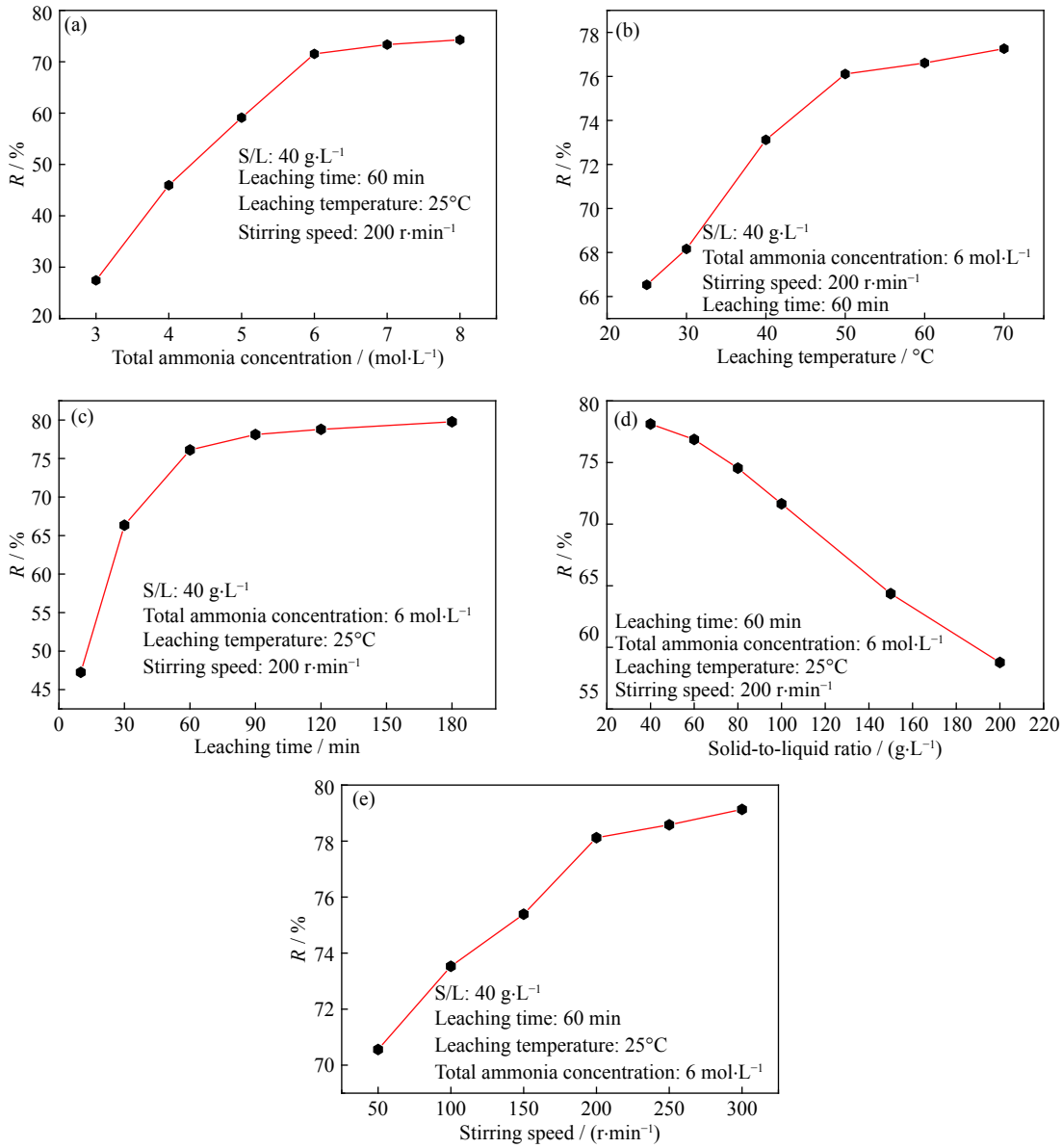

Fig. 8. Effect of leaching conditions on zinc-leaching rate: (a) total ammonia concentration; (b) leaching temperature; (c) leaching time; (d) solid-to-liquid ratio; (e) stirring speed.

200 r/min of stirring rate. In addition, the further increase from 6 to 8 mol/L in total ammonia concentration had no significant influence on the zinc-leaching rate, which meant that the total ammonia concentration of 6 mol/L was enough for extraction of zinc oxide from the roasted products in our study. Fig. 8(b) reveals that leaching temperature had a continuous positive influence on the zinc-leaching rate. The leaching rate increased gradually from 66.53% to 77.26% when the leaching temperature increased from 25 to 70°C, whereas the rate grew slowly at leaching temperatures > 50°C. In fact, in the context of industrial production, a higher leaching temperature would cause higher energy consumption, and higher volatility of ammonia would more seriously corrode equipment. Furthermore, it can be seen from Fig. 8(c) that the zinc-leaching rate almost reached its maximum of 78.12% within 90 min, but only 79.77% for 180 min, which indicated that most of the zinc oxide in the roasting products was extracted. Previous investigations showed that the fine granularity of reduced products has a large specific surface area and the NH_4^+ easily adheres to the surface of particles. Therefore, the dissolution of zinc oxide was rapid [34–35]. As displayed in Fig. 8(d), the solid-to-liquid ratio had a negative effect on the zinc-leaching rate. The zinc-leaching rate decreased rapidly from 78.12% to 58.78% as the solid-to-liquid ratio increased from 40 to 200 g/L. Therefore, The solid-to liquid ratio of 40 g/L was chosen in

order to obtain a higher zinc-leaching rate. Fig. 8(e) indicates that the zinc-leaching rate increased from 70.56% to 79.13% when stirring speed increased from 50 to 300 r/min. This was because the increasing stirring speed could increase the diffusion efficiency of zinc oxide and decrease the required level of activation energy in the dissolution reaction.

In conclusion, the optimal leaching conditions should be as follows: leaching temperature of 50°C, total ammonia concentration of 6 mol/L, leaching time of 90 min, 40 g/L of solid-to-liquid ratio, and a stirring speed of 200 r/min. Under optimal operating conditions, a 78.12% zinc-leaching rate was achieved.

4.2.2. Leaching residue analysis

The XRD patterns of the leaching residue that were obtained in the ammonia leaching process under the optimal conditions are shown in Fig. 9. They indicate that the main crystalline phases of the leaching residue were Fe_3O_4 and $ZnFe_2O_4$. Moreover, a small amount of zinc oxide (ZnO) was found in the leaching residue. In addition, the peaks of zinc oxide become weaker in the patterns after leaching, which meant that almost all zinc oxide was dissolved in ammonium-ammonia solution. It also can be inferred that the main reason for the limitation in the recovery ratio of zinc during the ammonia leaching was the under-composed $ZnFe_2O_4$.

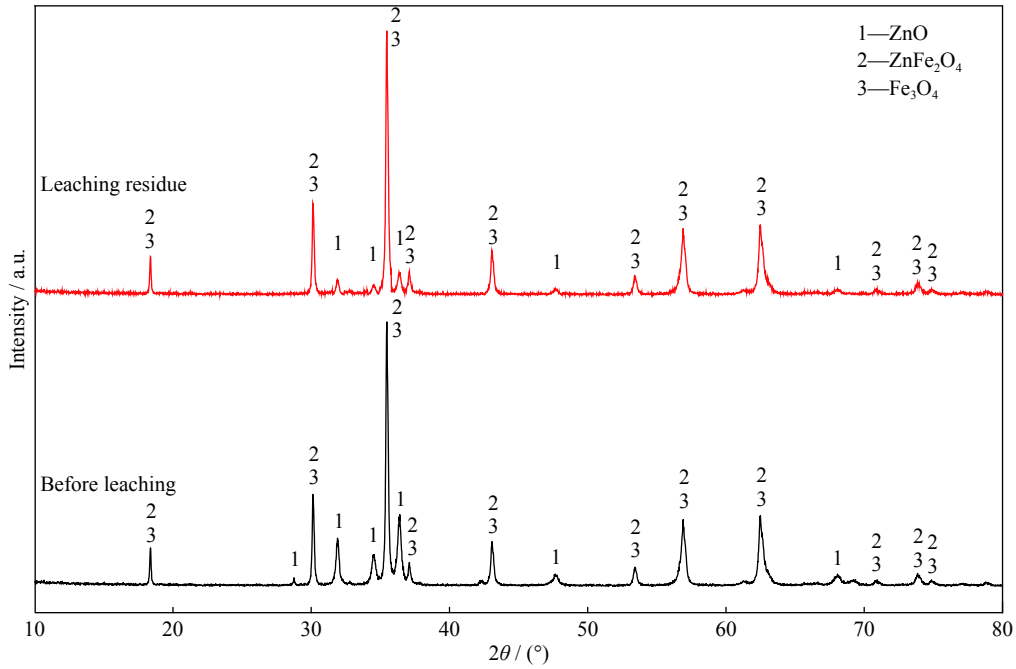

Fig. 9. XRD patterns of leaching residue and roasted product.

5. Conclusions

This study thermodynamically and experimentally confirmed that zinc ferrite ($ZnFe_2O_4$) could be selectively converted into ZnO and Fe_3O_4 by reduction roasting using CO gas. Increasing reduction atmosphere, roasting duration, and temperature, to some extent, are conducive to the decomposition of zinc ferrite. However, when these parameters exceed their optimum levels, a part of Fe_3O_4 or/and $ZnFe_2O_4$ will be over-reduced to FeO. The formed FeO can then react with ZnO to form the insoluble phase of $Zn(Fe_{0.85-x}Zn_xO)$, which is harmful to subsequent zinc extraction. Under the optimal conditions of reduction roasting, CO partial pressure of 25%, and a roasting temperature and duration of 750°C and 45 min, respectively, the conversion ratio of $ZnFe_2O_4$ reaches 86.43%. Zinc oxide can be extracted effectively from the reduction-roasted product with the ammonia leaching process. Zinc-leaching rate increases with increasing total ammonia concentration, leaching temperature, leaching time, and stirring speed, whereas it decreases with increasing solid-to-liquid ratio. A 78.12% zinc-leaching rate can be achieved under these optimal leaching conditions: leaching temperature and duration of 50°C and 90 min, respectively, total ammonia concentration of 6 mol/L, a solid-to-liquid ratio of 40 g/L, and a stirring speed of 200 r/min.

Acknowledgement

This work was financially supported by the National Key Basic Research and Development Program of China (No.

2014CB643403).

References

[1] T.T. Chen and J.E. Dutrizac, Mineralogical changes occurring during the fluid-bed roasting of zinc sulfide concentrates, *JOM*, 56(2004), No. 12, p. 46.

[2] W. Kim and F. Saito, Mechanochemical synthesis of zinc ferrite from zinc oxide and α-Fe_2O_3, *Powder Technol.*, 114(2001), No. 1-3, p. 12.

[3] Š. Langová and D. Matýsek, Zinc recovery from steel-making wastes by acid pressure leaching and hematite precipitation, *Hydrometallurgy*, 101(2010), No. 3-4, p. 171.

[4] B. Boyanov, A. Peltekov, and V. Petkova, Thermal behavior of zinc sulfide concentrates with different iron content at oxidative roasting, *Thermochim. Acta*, 586(2014), p. 9.

[5] X.L. Lin, Z.W. Peng, J.X. Yan, Z.Z. Li, J.Y. Hwang, Y.B. Zhang, G.H. Li, and T. Jiang, Pyrometallurgical recycling of electric arc furnace dust, *J. Cleaner Prod.*, 149(2017), p. 1079.

[6] Y.C. Li, H. Liu, B. Peng, X.B. Min, M. Hu, N. Peng, Y.Z. Yuang, and J. Lei, Study on separating of zinc and iron from zinc leaching residues by roasting with ammonium sulphate, *Hydrometallurgy*, 158(2015), p. 42.

[7] F. Zhang, C. Wei, Z.G. Deng, C.X. Li, X.B. Li, and M.T. Li, Reductive leaching of zinc and indium from industrial zinc ferrite particulates in sulphuric acid media, *Trans. Nonferrous Met. Soc. China*, 26(2016), No. 9, p. 2495.

[8] M. Hu, B. Peng, L.Y. Chai, Y.C. Li, N. Peng, Y.Z. Yuan, and D. Chen, High-zinc recovery from residues by sulfate roasting and water leaching, *JOM*, 67(2015), No. 9, p. 2005.

[9] Y.L. Zhang, X.J. Yu, and X.B. Li, Zinc recovery from franklinite by sulphation roasting, *Hydrometallurgy*, 109(2011), No. 3-4, p. 211.

[10] Y.C. Zhao and R. Stanforth, Extraction of zinc from zinc ferrites by fusion with caustic soda, *Miner. Eng.*, 13(2000), No. 13, p. 1417.

[11] T. Miki, R. Chairaksa-Fujimoto, K. Maruyama, and T. Nagasaka, Hydrometallurgical extraction of zinc from CaO treated EAF dust in ammonium chloride solution, *J. Hazard. Mater.*, 302(2016), p. 90.

[12] R. Chairaksa-Fujimoto, K. Maruyama, T. Miki, and T. Nagasaka, The selective alkaline leaching of zinc oxide from electric arc furnace dust pre-treated with calcium oxide, *Hydrometallurgy*, 159(2016), p. 120.

[13] N. Leclerc, E. Meux, and J.M. Lecuire, Hydrometallurgical extraction of zinc from zinc ferrites, *Hydrometallurgy*, 70(2003), No. 1-3, p. 175.

[14] T. Havlik, M. Turzakova, S. Stopic, and B. Friedrich, Atmospheric leaching of EAF dust with diluted sulphuric acid, *Hydrometallurgy*, 77(2005), No. 1-2, p. 41.

[15] P. Halli, J. Hamuyuni, M. Leikola, and M. Lundström, Developing a sustainable solution for recycling electric arc furnace dust via organic acid leaching, *Miner. Eng.*, 124(2018), p. 1.

[16] S.H. Yang, *Theory and Application Studies on Preparing High Purity Zinc in the System of Zn(II)–NH_3–NH_4Cl–H_2O* [Dissertation], Central South University, Changsha, 2003.

[17] R.X. Wang, M.T. Tang, S.H. Yang, W.H. Zhang, C.B. Tang, J. He, and J.G. Yang, Leaching kinetics of low grade zinc oxide ore in NH_3–NH_4Cl–H_2O system, *J. Cent. South Uni. Technol.*, 15(2008), No. 5, p. 679.

[18] D.K. Xia and C.A. Pickles, Kinetics of zinc ferrite leaching in caustic media in the deceleratory period, *Miner. Eng.*, 12(1999), No. 6, p. 693.

[19] B.A. Zeydabadi, D. Mowla, M.H. Shariat, and J.F. Kalajahi, Zinc recovery from blast furnace flue dust, *Hydrometallurgy*, 47(1997), No. 1, p. 113.

[20] M.D. Turan, H.S. Altundoğan, and F. Tümen, Recovery of zinc and lead from zinc plant residue, *Hydrometallurgy*, 75(2004), No. 1-4, p. 169.

[21] X. Wang, D.J. Yang, S.H. Ju, J.H. Peng, and X.H. Duan, Thermodynamics and kinetics of carbothermal reduction of zinc ferrite by microwave heating, *Trans. Nonferrous Met. Soc. China*, 23(2013), No. 12, p. 3808.

[22] M. Li, B. Peng, L.Y. Chai, N. Peng, H. Yan, and D.K. Hou, Recovery of iron from zinc leaching residue by selective reduction roasting with carbon, *J. Hazard. Mater.*, 237-238(2012), p. 323.

[23] H. Yan, L.Y. Chai, B. Peng, M. Li, N. Peng, and D.K. Hou, A novel method to recover zinc and iron from zinc leaching residue, *Miner. Eng.*, 55(2014), p. 103.

[24] J.W. Han, W. Liu, W.Q. Qin, K. Yang, D.W. Wang, and H.L. Luo, Innovative methodology for comprehensive utilization of high iron bearing zinc calcine, *Sep. Purif. Technol.*, 154(2015), p. 263.

[25] N. Peng, B. Peng, L.Y. Chai, M. Li, J.M. Wang, H. Yan, and Y. Yuan, Recovery of iron from zinc calcines by reduction roasting and magnetic separation, *Miner. Eng.*, 35(2012), p. 57.

[26] J.W. Han, W. Liu, W.Q. Qin, B. Peng, K. Yang, and Y.X. Zheng, Recovery of zinc and iron from high iron-bearing zinc calcine by selective reduction roasting, *J. Ind. Eng. Chem.*, 22(2015), p. 272.

[27] G. Yu, N. Peng, L. Zhou, Y.J. Liang, X.Y. Zhou, B. Peng, L.Y. Chai, and Z.H. Yang, Selective reduction process of zinc ferrite and its application in treatment of zinc leaching residues, *Trans. Nonferrous Met. Soc. China*, 25(2015), No. 8, p. 2744.

[28] R. Chairaksa-Fujimoto, Y. Inoue, N. Umeda, S. Itoh, and T. Nagasaka, New pyrometallurgical process of EAF dust treatment with CaO addition, *Int. J. Miner. Metall. Mater.*, 22(2015), No. 8, p. 788.

[29] Beijing General Research Institute of Mining and Metallurgy, *Chemical Phase Analysis*, Metallurgical Industry Press, Beijing, 1979.

[30] M. Li, *Fundamental Research on Selective Reduction of Zinc Calcine and Separation of Zinc and Iron* [Dissertation], Central South University, Changsha, 2013.

[31] C.C. Wu, F.C. Chang, W.S. Chen, M.S. Tsai, and Y.N. Wang, Reduction behavior of zinc ferrite in EAF-dust recycling with CO gas as a reducing agent, *J. Environ. Man-*

age., 143(2014), p. 208.

[32] H. Yan, *Treatment of Zinc Leaching Residue Based on the Selective Reduction of Zinc Ferrite* [Dissertation], Central South University, Changsha, 2014.

[33] Y.L. Sui, Y.F. Guo, T. Jiang, and G.Z. Qiu, Reduction kinetics of oxidized vanadium titano-magnetite pellets using carbon monoxide and hydrogen, *J. Alloys Compd.*, 706(2017), p. 546.

[34] W. Chen, Y.F. Guo, F. Chen, T. Jiang, and X.D. Liu, The extraction of zinc from willemite by calcified-roasting and ammonia-leaching process based on phase reconstruction, [in] *the 7th International Symposium on High-Temperature Metallurgical Processing*, *Nashville*, 2016, p. 109.

[35] F. Chen, W. Chen, Y.F. Guo, S. Wang, F.Q. Zheng, T. Jiang, Z.Q. Xie, and L.Z. Yang, Thermodynamics and phase transformations in the recovery of zinc from willemite, *Int. J. Miner. Metall. Mater.*, 25(2018), No. 12, p. 1373.